"CAROL DAVILA" UNIVERSITY OF MEDICINE AND PHARMACY BUCHAREST
DOCTORAL SCHOOL
FIELD OF MEDICINE

Doctoral Thesis Summary

Research on rhinosinusal variational anatomy

Scientific leader

Prof.Univ.Dr.Med.Dr.Biol.Dr.Habil.

Rusu Mugurel Constantin

PhD student

dr.Alexandru Nicolae Mureşan

Bucharest, 2024

CONTENTS

List of published scientific papers

Publication	Journal indexing	Type of publication/author	Chapters Thesis
Muresan AN, Dandoczi CA, Tudose RC, Hostiuc S, Rusu MC. Anatomical Possibilities of the Alveolar Bone at the UPEPr Second Premolar Level. *Medicina (Kaunas)* 2024; **60**(5).	ISI WOS SCIE IF 2.4	Article principal author	8 pag.57-70
Muresan AN, Rusu MC, Radoi PM, Toader C. Patterns of Pneumatization of the Posterior Nasal Roof. *Tomography* 2022; **8**(1): 316-28.	ISI WOS SCIE IF 1.9	Article principal author	4 pag.23-38
Muresan AN, Mogoanta CA, Stanescu R, Rusu MC. The sinus septi nasi and other minor pneumatizations of the nasal septum. *Rom J Morphol Embryol* 2021; **62**(1): 227-31.	ISI WOS SCIE IF 1.033	Article principal author	7 pag.48-56
Rusu MC, **Muresan AN**, Dandoczi CA, Vrapciu AD. Middle meatal nasal recesses of the maxillary sinuses and dangerously modified nasal anatomy. *Anatomy & cell biology* 2024.	ISI WOS ESCI IF 1.4	Case Report co-author	6 pag.43-49
Geamanu A, Rusu MC, **Muresan AN**, Vrapciu AD. The Ethmomaxillary Sinus-A False Duplicate Maxillary Sinus. *The Journal of craniofacial surgery* 2024; **35**(5): e458-e61.	ISI WOS SCIE IF 1.0	Case Report co-author	11 pag.92-95
Ilie AC, Jianu AM, Rusu MC, **Muresan AN**. Anatomical Changes in a Case with Asymmetrical Bilateral Maxillary Sinus Hypoplasia. *Medicina (Kaunas)* 2022; **58**(5): 564.	ISI WOS SCIE IF 2.6	Case Report principal author	11 pag.92

List of abbreviations in the text

EB - ethmoid bulla;

ACF – anterior cranial fossa;

AEC - anterior ethmoid cell;

ANC - Agger Nasi cell;

CBCT – Cone-Beam Computed Tomography;

CEP – cribriform ethmoidal plate;

CF – canine fossa;

CG – crista galli;

EI – ethmoidal infundibulum;

EMS – ethmomaxillary sinus;

CF – frontal ethmoidal cells;

FR – frontal recess;

FS – frontal sinus;

INM – inferior nasal meatus;

INT – inferior nasal turbinate;

MNM – middle nasal meatus;

MNT – middle nasal turbinate;

MS – maxillary sinus;

MSH – maxillary sinus hypoplasia;

NF – nasal fossa;

NS – nasal septum;

PEC - posterior ethmoid cells;

PEP – perpendicular ethmoidal plate;

RMC – retromaxillary cell;

SphenS – sphenoidal sinus;

SH – semilunar hiatus;

SNM – superior nasal meatus;

SNT – superior nasal turbinate;

SSN – sinus septi nasi;

UP – uncinate process.

Introduction

The exploration of rhinosinusal anatomy is now greatly facilitated by modern imaging techniques. Of these, Cone Beam Computed Tomography (CBCT), which is mainly used in dentistry, allows detailed rhinosinusal anatomical, morphological and morphometric evaluation, which is an advantage for anatomical research.

I pursued exploratory research directions of the nasal walls and maxillary sinus less reflected in the specialized literature and specific treatises. The research results support that the variational possibilities of rhinosinonasal anatomy go beyond the limits of usual undergraduate anatomy but are appreciated in relation to it. Anatomical variations relevant in practice are not usually discussed in usual anatomy programs and graduates are not familiar with them [1]. Modern imaging exploration has the possibility of personalized anatomical exploration. My PhD thesis makes a number of contributions to rhinosinusal anatomy. I demonstrated that the base of the maxillary alveolar process can be localized not only inferior to the maxillary sinus, but also inferior to the inferior meatus of the nasal fossa. I pointed out that the canine fossa, which is associated in the literature exclusively with the anterolateral wall of the maxillary sinus, can localize to the inferior meatal wall. I detailed the possibilities of pneumatization of the nasal roof and septum, respectively. The nasal recess of the maxillary sinus that I report is the first such morphologic evidence.

1 General part of the doctoral thesis

In the general part of the thesis I present data from the literature on the morphogenesis of the rhinobasis, elements of rhinoanatomy and elements of morphogenesis and anatomy of the paranasal sinuses.

2 Personal part of the doctoral thesis

2.1 Variational anatomy of the nasal roof

Currently available preoperative diagnostic tools allow a good therapeutic efficiency and lead to possible minor iatrogenic lesions [2]. The basis of minimizing iatrogenicity in the surgical field is the understanding and knowledge of microsurgical anatomy [2].

Laterally, the cribriform ethmoidal plate (CEP) reaches the level of the ethmoid cells. Although the sphenoid body is pneumatized, as are the ethmoid cells, the anatomical possibilities of ethmoid or sphenoid extensions above or in the thickness of the CEP have not been previously rigorously documented anatomically. I therefore decided to perform a retrospective study on a relevant batch of CBCT scans [3]. I retrospectively documented 175 CBCT records, 13 cases were excluded, so I documented 162 CBCT records from 55 men and 107 women. Different anatomic patterns were defined. These were grouped into four types: type I: absence of pneumatization at the posterior end of the CEP; type II: ethmoid origin of CEP pneumatization; type III: sphenoid origin of CEP pneumatization; type IV: sphenoethmoid origin, from an Onodi cell, of CEP pneumatization. Each type (II-IV) was classified into two subtypes, either "a" intracranial, with pneumatization localized above the CEP, or "b" intranasal, with pneumatization localized in the thickness or below the CEP. Each subtype showed three patterns: "1": unilateral pneumatization of the nasal roof; "2": extended contralateral pneumatization of the nasal roof; "3" bilateral pneumatization, with similar origin. This resulted in variables that were recorded and analyzed using the Microsoft Excel program: (1) type I - lack of pneumatization at the posterior end of the CEP; (2) type II - CEP pneumatization of ethmoid origin, from a posterior ethmoid cell: subtype IIa: intracranial ethmoid pneumatization, above the CEP: IIa1: unilateral restricted; IIa2: contralateral extended; IIa3: bilateral; subtype IIb: intranasal ethmoid pneumatization, replacing the posterior end of the CEP: IIb1: unilateral restricted; IIb2: contralateral extended; IIb3: bilateral; (3) type III - ECL pneumatization of sphenoid origin, from a sphenoid sinus: subtype IIIa: intracranial sphenoid pneumatization, above the ECL: IIIa1: unilateral restricted; IIIa2: contralateral extended; IIIa3: bilateral; subtype IIIb: intranasal sphenoid pneumatization, replacing the posterior end of the ECL: IIIb1: unilateral restricted; IIIb2: contralateral extended; IIIb3: bilateral; (4) type IV - CEP pneumatization of sphenethmoid origin, from an Onodi cell: subtype IVa: intracranial sphenethmoid pneumatization, above the CEP: IVa1: unilaterally restricted; IVa2: extended contralaterally; IVa3: bilateral; subtype IIb: intranasal sphenoethmoid pneumatization, replacing the posterior end of the CEP: IVb1: unilaterally restricted; IVb2: extended contralaterally; IVb3: bilateral.

There were highlighted different anatomic patterns of pneumatization of the posterior nasal roof, except for type IIb2 (contralateral extended ethmoid recess below the CEP) and type IVa (extended sphenoethmoid Onodi cells above the CEP).

Type I CEP, i.e. non-pneumatized CEP, was present in 91 out of 162 cases (56.17%), 28 male and 63 female. Thus, in the other 43.83% of cases we found different patterns of pneumatization of the posterior nasal roof, either recesses added above the CEP (subtype "a") or replacing the posterior end of the CEP (subtype "b").

Nasal roof recesses of ethmoid origin were localized at the posterior end of the PEC in 33/162 cases (20.37%), uncombined or in combinations. In three cases (1.85%), one male and two females, we found type IIa1 uncombined - unilateral ethmoidal pneumatizations extending unilaterally above the CEP. Uncombined type IIa2 was found in two cases (1.23%), in males and females. Uncombined type IIa3 was found in one male case (0.61%). Uncombined type IIb1, unilateral ethmoid pneumatization within or below the CEP, was found in 8/162 cases (6.06%). In 12/162 cases (7.4%), three males and nine females, uncombined type IIb3 was found, i.e. bilateral intranasal ethmoidal pneumatizations replacing the posterior end of the CEP. In two male cases (2/162, 1.23%) a combination of types IIa1 and IIa2 was found. In one female case (1/162, 0.61%), a combination of types IIa3 and IIIa2 was found, thus bilateral ethmoid pneumatization above the CEP fed from both ethmoid labyrinths, with added contralateral extensive recess of the left sphenoid sinus. In another female case (0.61%), combined types IIa1 and IIIa1 were found, i.e. unilateral ethmoid and sphenoid pneumatizations above the posterior end of the CEP. Another female case (0.61%) had a combination of types IIa1 and IIIa2, thus unilateral ethmoidal pneumatization of the CEP, but extensive sphenoid pneumatization contralateral to the nasal roof. In one male case (0.61%) the combination of types IIb3 and IIIb2 was found, thus bilateral ethmoidal pneumatization under the CEP fed from both ethmoidal labyrinths, with added contralateral extended recess of the left sphenoid sinus. In another male case (0.61%) the combination of IIb1+IVb2 was found: on the left side a posterior ethmoid cell extended below the CEP and a right Onodi cell extended contralateral below the CEP.

Different types of sphenoid pneumatizations of the posterior end of the posterior end of the PEC were found in 37/162 cases (22.83%), uncombined or in combinations. Unilateral sphenoid pneumatization above the CEP (type IIIa1 non-combined) was found in three cases (1.85%%), one male and two females. Type IIIa2 uncombined, contralateral extended sphenoid recess contralateral above the CEP, was found in 5/162 cases (3.08%), one male and four females. Uncombined type IIIa3, bilateral sphenoid recession above the CEP, was found in one male case (1.23%). Uncombined type IIIb1 was found in 14/162 cases (8.64%), 6 males and 8 females. Uncombined type IIIb2, with extensive sphenoid recess contralateral

below the CEP, was found in 5/162 cases (3.08%), three males and two females. Type IIIb3, bilateral sphenoid recesses in or below the CEP, was found in only 2/162 male cases (1.23%). In three cases (1.85%) we identified the combination IIIb1+IVb1, thus unilateral sphenoid extensions and Onodi below the CEP, respectively.

Type IVb (extensive recesses from Onodi cells under CEP), was found in ten cases. In four of these, combinations of types that have already been described in this section were found. Therefore, in only 6/162 cases (3.7%) uncombined IVb types were found. Uncombinated type IVb1, unilateral extension of an Onodi cell within or below the CEP, was found in 2/162 cases (1.23%). In 3/162 cases (1.85%), uncombinated type IVb2, with contralateral extension of the Onodi cell into the nasal roof, was found. In only one case, female (0.61%), was type IVb3 uncombined - bilateral Onodi cells extending recess bilaterally under the CEP.

Van Alyea published in 1939 a study by dissection of 100 ethmoid labyrinths [4]. He discussed that ethmoid cells have a tendency to expand and fill any available space [4]. Such extensions are either usual or unusual [4]. Van Alyea called those that drain superiorly from the superior nasal turbinate "postreme cells" [4]. Such postreme cells have been observed invading the sphenoid sinus, optic canal, or extending medially to reach the nasal septum or even the opposite side [4]. However, Van Alyea did not explicitly note CEP pneumatization by such postreme ethmoid cell recesses [3].

Van Alyea detailed the anatomy of SphenS as early as 1941 [5]. He described that the SphenS is not confined to the body of the sphenoid bone with and that sinus recesses into adjacent bony processes occur with regularity 5. Often, the recesses extending anteriorly from the sphenoid sinuses are large enough to occupy a considerable portion of the ethmoid field [5]. The "medial anterior (septal)" recess of the SphenS has been enumerated by Van Alyea, but it has not been observed that the sinus can also extend above the NF to cancel or replace the posterior end of the CEP, as we observed in the present study. Such anterior supranasal recesses anterior to the SphenS are commonly seen in computed tomography scans but are overlooked [6].

The anatomic details of the sphenoid body include several bony extensions that may project anteriorly over the ethmoid: (a) the medial, unpaired one is the ethmoid spine of the sphenoid, usually triangular and with the apex pointing toward the CG; (b) the paired lateral processes, if present, are the minimal sphenoid wings of Luschka [2]. A pneumatized ethmoid spine would result in a pneumatized posterior nasal roof overlying the CEP. A wide anterior

septal recess of the SphenS could result in adjacent pneumatizations below the posterior end of the CEP [3].

Onodi cells occur in 3.4-51% of individuals, as previously documented [7]. An Onodi cell is a posterior ethmoid cell that has an intimate relationship with the optic nerve (II) [7,8]. However, when a medial recess of an Onodi cell covers the nasal fossa, it will also be in close relation to the olfactory bulb above the CEP [3].

Different studies have observed the variational anatomy of the nasal fossa walls [9-18]. However, these studies have not shown the variable patterns of nasal roof pneumatization that I have described here [3]. Typically only the fact that the nasal cavity roof is formed by CEPs is commonly indicated [19]. Gore (2019) reported a "supraseptal cell of the ethmoid sinus" corresponding to type IIa1 pneumatization of CEPs in my research [3]. The author considered this finding to be the first case of this type reported in the literature [20]. He noted that "in documenting hundreds of preoperative maxillofacial CT scans" that case "had the only example of this particular ethmoid cell" [20]. This is interesting because we found different pneumatized CEP patterns in less than 200 cases [3].

Olfactory sensitivity is important for MSell, emotion formation and memory [21]. Olfactory dysfunction can have a profound impact on quality of life and mental status and is associated with depression [21]. Thus, olfaction should be considered during endoscopic skull base surgical procedures where there is a risk of odor loss in normoMSic patients [21]. Loss of odor after endoscopic skull base surgery may theoretically be due to direct trauma, inflammatory changes, or obstruction [21]. Pressure or injury to the olfactory neuroepithelium may cause temporary or permanent loss of MSell [21]. Inflammatory changes in the olfactory mucosa and nasal obstructions may play a role in producing hypoMSia [21].

A pneumatized roof of the posterior nasal fossa is a pneumatized ceiling of sphenoethmoid recess [3]. The SphenS ostium is located either in the posterior wall of this recess or in lateral wall [22]. Care should be taken when the ostium of the sphenoid sinus is approached endoscopically to avoid penetration of a pneumatized ceiling of the sphenoethmoid recess, i.e. a pneumatized posterior end of the CEP [3]. The vertical level of the CEP is individually variable and, if crossed, could subsequently lead to encephaloceles and cerebrospinal fluid leakage [23].

The endoscopic endonasal transcribriform endoscopic approach is a reliable strategy in the treatment of various pathologies of the anterior skull base, such as meningiomas of the

olfactory groove, meningoencephalocele, esthesioneuroblastomas, schwannoomas or other sinus tumors [24]. On a case-by-case basis, it could be converted to a transcranial-endonasal endonasal transcribriform transcranial-endonasal approach [24]. Such transcribriform approaches should document in advance whether or not the CEP has an added pneumatic pattern in order to avoid, if possible, an unnecessary opening of a paranasal pneumatic space [3].

2.2 Giant Onodi Cell

The anatomy of the ethmoidal labyrinth is extremely variable. Posterior ethmoid air cells that extend posteriorly to override the sphenoidal sinus (SphS) and to contact the optic canals are sphenoethmoidal or Onodi's cells (OCs). Such OCs modify the typical surgical corridors. The archived Cone Beam Computed Tomography (CBCT) files of a 54 y.o. female case were retrospectively studied anatomically. The left SphS was of postsellar type. It extended contralaterally and thus reached both cavernous sinuses. The right SphS was of presellar type. Both SphSs were opened anteriorly into the nasal fossa above the superior nasal turbinates. A left giant OC extended posteriorly into the sphenoidal body and was overriding both SphSs, contacting both optic canals. It directly drained anteriorly into the nasal fossa, at 7.27 mm inferior to the cribriform ethmoidal plate. The ostium of the left SphS was inferior to that OC. It also crossed above the nasal septum and roofed both nasal fossae. Conclusions: A giant unilateral OC could override both SphSs and contact both optic canals. The drainage patterns of such large OCs and the SphS are different, allowing for the anatomical distinction between them.

2.3 Variational anatomy of the lateral nasal wall – the nasal recess of the maxillary sinus

Pneumatisation of the maxillary sinus (MS) is variable. Different recesses expand the MS within neighbour structures or spaces. The archived Cone Beam Computed Tomography file of a 54 y.o. female was retrospectively evaluated anatomically. The significant findings were the nasal or retrobullar recesses of the MSs (NRMS). The right MS was divided by an intrasinus septum into two intercommunicating chambers, one MSaller antero-medial and the other larger, postero-lateral. A large NRMS of the postero-lateral chamber was extended into the lateral nasal wall, superior to the middle turbinate. The highest depth of that NRMS was 11.0 mm. The ethmoidal bulla was applied on the anterior side of that NRMS, and the tip of the NRMS reached within the basal lamella of the middle turbinate. The left MS was almost entirely divided into antero-medial and postero-lateral chambers by an oblique septum

inserted superiorly on the infraorbital canal. A NRMS of 12.5 mm depth extended from its postero-lateral chamber. It had two medial pouch-like ends, one beneath the ethmoidal bulla and the other on the anterior side of the basal lamella of the middle turbinate. Additional anatomical findings in the present case were the uncinate bulla, infraorbital recesses of the MS, maxillary recess of the sphenoidal sinus, and atypical posterior insertions of the superior nasal turbinates, maxillo-ethmoido-sphenoidal and ethmoido-sphenoidal. The NRMS is a novel finding and could lead to erroneous endoscopic corridors if not documented before the interventions [25].

2.4 Variational anatomy of the pneumatizations of the nasal septum

The nasal septum (NS) mainly consists of the perpendicular plate of the ethmoid bone (PEP) and the vomer. The PEP reaches anteriorly the nasal part of the frontal bone and posteriorly joins the sphenoidal rostrum of the body of sphenoid. The PEP is continuous above the CEP with the crista galli (CG). Quite recently, Mladina et al. used 93 dry skulls which they scanned in cone-beam computed tomography (CBCT) to observe the pneumatizations of the NS [26]. They found in 34.4% a pneumatization of the PEP, which they termed "sinus septi nasi" (SSN) [26]. As the respective authors wrote, "this is the first anatomical study on the incidence of SSN in human skulls" [26]. They hypothesized in conclusion that the SSN could be derived either from the frontal sinus (FS), or from the sphenoidal sinus (SphenS), or from the vomeronasal organ. This is because the origin of those SSN was not explicitly documented in that study. It is important to note that although Mladina et al. [26] used a "skull collection" of an Institute of Anatomy, evidence in most figures includes bone and soft tissues. Soft tissues, such as orbit content and covering mucosae, could not be scanned in dry skulls. As the study of Mladina et al. [26] was indicated by the authors as a pioneering one, further studies have to evaluate the anatomy of the NS pneumatizations on CBCT scans of living patients. We therefore aimed doing so, to observe the anatomical possibilities of NS pneumatizations, i.e., the prevalence and sources of the PEP pneumatization [26].

A retrospective CBCT study of the archived records of 190 patients explored for dental medical purposes was performed. The following variables were recorded in a Microsoft Excel file, further performing descriptive statistics: (1) lack of SN pneumatizations; (2) pneumatized CG; (3) septal extensions of the FS; (4) posterior septal pneumatizations of sphenoid origin; (5) ethmoidal sources of PEP pneumatization. A critical review of specific literature was also performed [26].

In 19 cases of males and 27 of females we did not record pneumatization of the nasal septum. Therefore, 46/171 (26.9%) cases were classified as nil for septal pneumatizations. The remaining cases (73.1%) had various septal pneumatizations extending from neighboring airspaces as follows. GC pneumatizations were found in 4 male and 8 female cases, thus in 12/171 cases (7.01%). All these pneumatizations extended from the frontal sinus. In three male cases, the source of sinus cristae galli was the right frontal sinus, and in another male case the CG pneumatization extended from the left FS. In the female cases, the origin of the sinus cristae galli originated from the right frontal sinus in three cases and from the left frontal sinus in five cases. The maximum transverse transverse diameter of the sinus cristae galli was measured in these cases. An average value of 4.085 mm was found. The values ranged from a minimum of 2.37 mm to a maximum of 5.25 mm. The frontal sinuses had minor extensions anterior to the PEP in 3 males and 10 females, i.e. in 13/171 cases (7.6%). In 8 of these 13 cases (61.53%), these extensions originated from the right frontal sinus, and in the remaining 5 cases (38.47%) from the left frontal sinus. Pneumatizations of the sphenoid rostrum extending posterior to the PEP were found in 32 cases in males, being single in 31 cases and double in one case. In female cases, single pneumatizations of the rostrum were found in 83 cases, while double pneumatizations of the rostrum were found in 7 cases. Therefore, out of 171 cases, 122 (71.34%) had sphenoid pneumatizations of the posterior nasal septum. All double pneumatizations of the sphenoid rostrum extended from both left and right sphenoid sinuses. In 18 male cases, the rostrum was pneumatized from the left sphenoid sinus, and in 13 cases - from the right sphenoid sinus. In 47 female cases, the rostrum was pneumatized from the left sphenoid sinus and in 36 cases from the right. Two male cases were found with pneumatizations of the PEP supplied from the ethmoidal air cells, one anterior and one posterior, respectively. In female cases, single pneumatizations of the rostrum were found in 83 cases, while double pneumatizations of the rostrum were found in 7 cases. Therefore, out of 171 cases, 122 (71.34%) had sphenoid pneumatizations of the posterior nasal septum. All double pneumatizations of the sphenoid rostrum extended from both left and right sphenoid sinuses. In 18 male cases, the rostrum was pneumatized from the left sphenoid sinus, and in 13 cases - from the right sphenoid sinus. In 47 female cases, the rostrum was pneumatized from the left sphenoid sinus and in 36 cases from the right. Two male cases were found with pneumatizations of the PEP supplied from the ethmoidal air cells, one anterior and one posterior, respectively. Four female cases were recorded with pneumatizations of the PEP, two from anterior ethmoid cells, one from a posterior ethmoid cell and one from the CG. In the latter case, the left frontal sinus extended and pneumatized the nasal part of the frontal bone, CG and PEP. Measurements

of this sinus septi nasi revealed a sagittal extension of 25.37 mm, a transverse dimension of 5.75 mm and a height of 13.58 mm.

The anatomic variations of the paranasal sinuses are well known. The dimensions (length, width and depth) of the pneumatization of the crista galli and nasal septum cannot be standardized due to the insufficient number of studies in the literature [27]. Pneumatization of the nasal septum has aroused great research interest in recent years [28]. Sinus septum pneumatization appears, according to a recent systematic review [27], in very few studies [26,30-36]. Gore first reported a "supraseptal ethmoid cell" which he demonstrated to be an anterior ethmoid cell extended anteriorly above the PEP 20. In the present study, in 171 cases we found 3 (1.75%) such ethmoid cells [26]. Thus demonstrating that the variant reported by Gore in 2019 is rare. However, the term 'supraseptal extension, or recess' of an ethmoid cell better describes this variant [26]. This is because Gore's term "supraseptal ethmoidal cell" suggests that the main airspace is supraseptal, not just the supero-medial recess of the ethmoidal cell in question [26]. Furthermore, we found such supraseptal but posterior ethmoid cell recesses in 2/171 cases (1.16%) [26]. Therefore, one could conclude that, although rare, any ethmoid cell could extend a supraseptal supero-medial recess into the nasal and superior roof of the nasal and superior PEP [26].

2.5 Topographic variability of the antral floor at the level of the second upper premolar

The inferior wall of the MS is curved and is formed by the lower 1/3 of the medial wall of the MS and the buccoalveolar wall; the antral floor is realized by the alveolar process of the maxilla [29]. Studies on the antral floor focus on specific dentoantral relationships, starting from the unique premise that the maxillary alveolar bone has superiorly only the antral floor [29-32]. I started in my research from the assumption of variability of the topographic relationships superior to the palatal segment of the maxillary alveolar bone respectively [33]. The aim of the research was thus to assess in retrospective groups whether the alveolar bone may have different superior ratios in its palatal side, and not exclusively with MS. I used an archived retrospective batch of archived CBCT head scans of 150 cases. There were 62 male cases, 2 cases were excluded, 60 were included in the study. There were 88 female cases, 3 cases were excluded, 85 were included in the study. Thus I followed anatomic variables in a group of 145 cases. I defined four possible topographic types of the maxillary alveolar base, as follows: type 1 - exclusively antral base; type 2 - antral alveolar base, with palatal recess of the antral floor interposed between the alveolar bone and the nasal fossa on that side; type 3 - antral and nasal

alveolar base, participating directly in both the antral floor and the nasal wall (floor); type 4 - exclusively nasal alveolar base. On the orthoradial sections at the level of the upper second premolar on each side of the median plane I measured for type 2: orthoradial width of the alveolar bone (process); rectilinear width of the antral plane; maximum antropalatal depth of the palatal recess of the MS. On the orthoradial sections at the level of the upper second premolar on either side of the median plane I measured for type 3: the width of the alveolar base, considered either as the buccopalatal thickness of the alveolar process (dentate) or that of the alveolar bone (edentulous) in the middle 1/3; the straight width of the antral plane; the straight width of the alveolonasal plane. I recorded the following variables (vertical topography) for types 1- 3: "a" - the antral plane higher than the nasal plane; "b" - the antral plane at the same level as the nasal plane; "c" - the antral plane lower than the nasal plane (alveolar recess of the MS). I classified the palatal recesses of the antral plane as open (O) when they communicated widely with the antral cavity and closed (C) when they were almost completely separated from the main antral cavity. I used a series of statistical tests to assess the results obtained. To assess the number of cases of each variant I used frequencies and gender distribution. To assess significant associations between qualitative variables I used Pearson Chi2 test. I used ANOVA tests to identify whether differences exist on morphometric determinations. I applied Pearson correlation test to assess two-tailed associations between measured variables. I used the SPSS v28 program for iOS system to perform statistical analyses.

I documented antral floor types and subtypes bilaterally in the maxillary second premolar. On the right side, type 1c antral floor type 1c (42.76%) prevailed in the maxillary second premolar. On the left side, type 1c antral floor type 1c (38.62%) prevailed in the maxillary second premolar. In the total of 290 unilateral determinations, type 1a was determined in 4.48% of cases, type 1b in 22. 07% of the cases, type 1c in 40.69% of the cases, types 2bO and 2cC in only 0.34% of the cases each, type 2cO in 12.76% of the cases, type 3a in 10.69% of the cases, type 3b in 3.45% of the cases, type 3c in 2.07% of the cases and type 4 in 3.10% of the cases. Thus, type 1 was detected in 195/290 sinuses (67.24%). On the right side, type 1 was identified in 68.28%. On the right side, type 1 was identified in 66.21%. On the right side I did not register types 2bO and 2cC. In type 2cO on the right side (17 cases) the orthoradial width of the alveolar bone averaged 7.16 mm (SD: 3.72 mm), the rectilinear width of the antral plane averaged 8.21 mm (SD: 1.38 mm) and the depth of the palatal recess averaged 4.08 mm (SD: 2.31 mm). In type 3a on the right side (17 cases) the orthoradial width of the alveolar bone averaged 8.03 mm (SD: 1.64 mm), the rectilinear width of the antral plane averaged 4.55 mm

(SD: 1.4 mm) and the rectilinear width of the alveolonasal plane averaged 7.83 mm (SD: 2.2 mm). In type 3b on the right side (6 cases) the orthoradial width of the alveolar bone averaged 8.55 mm (SD: 2.26 mm), the rectilinear width of the antral plane averaged 7.03 mm (SD: 3.02 mm) and the rectilinear width of the alveolonasal plane averaged 4.78 mm (SD: 0.59 mm). In type 3c on the right side (3 cases) the orthoradial width of the alveolar bone averaged 9.66 mm (SD: 1.26 mm), the rectilinear width of the antral plane averaged 9.74 mm (SD: 0.94 mm) and the rectilinear width of the alveolonasal plane averaged 6.18 mm (SD: 1.19 mm). On the left side we recorded all subtypes 2 and 3. In type 2bO (one case) the orthoradial width of the alveolar bone averaged 9.65 mm, the rectilinear width of the antral plane averaged 10.2 and the depth of the open palatal recess averaged 2.25 mm.

In type 2cC (one case), the orthoradial width of the alveolar bone was 8.5 mm, the rectilineal width of the left antral plane was 8.5 mm and the depth of the palatal recess was 6.33 mm. Type 2cO was present on the left in 20 cases. The orthoradial width of the alveolar bone was 7.73 mm (SD: 4.1 mm), the rectilinear width of the antral plane was 9.07 mm (SD: 1.9 mm) and the depth of the palatal recess was 3.87 mm (SD: 1.97 mm). On the left side type 3a was identified in 14 cases. The orthoradial width of the alveolar bone averaged 8.45 mm (SD: 1.24 mm), the rectilinear width of the antral plane averaged 4.9 mm (SD: 1.66 mm) and the rectilinear width of the alveolonasal plane averaged 7.35 mm (SD: 2.36 mm). In type 3b, on the left side (4 cases), the orthoradial width of the alveolar bone averaged 6.95 mm (SD: 0.92 mm), the rectilinear width of the antral plane averaged 5.9 mm (SD: 1.39 mm) and the rectilinear width of the alveolonasal plane averaged 4.93 mm (SD: 1.54 mm). In type 3c, on the left side (3 cases), the orthoradial width of the alveolar bone averaged 9.5 mm (SD: 1.09 mm), the rectilinear width of the antral plane averaged 8.83 mm (SD: 2.89 mm) and the rectilinear width of the alveolonasal plane averaged 4.86 mm (SD: 1.84 mm). I identified that types 1 and 2, respectively, exhibited a strong level of statistically significant bilateral symmetry (Pearson Chi2 = 86.42, p<.001). Type 3 was correlated bilaterally equally with type 1 and with contralateral type 3. Bilateral symmetry for determined types 1-3 was stronger in males (Pearson Chi2 = 47.83, p<.001) than in females (Pearson Chi2 = 56.96, p<.001). We found no statistically significant associations between sex and unilateral anatomic type. The ANOVA test indicated that for alveolar base width on the right side, there were no statistically significant differences in this determination. There were, however, statistically significant differences (larger swings in values) for the right-sided width of both the antral (F = 17.26, p<.001) and alveolonasal (F = 9.82, p<.001) planes. There were also statistically significant differences on

the left side for the antral plane (F = 9.72, p<.001) and for the alveolonasal plane (F = 5.08, p=.001). Correlation tests showed a negative linear association (Pearson = -0.453, p=.002) between the dimensions of the antral plane and the alveolonasal plane on the right side. Similarly, we also obtained a negative association between the two variables on the left side (Pearson = -0.499, p<.001). We also found a positive bilateral positive association between the size of the antral plane (Pearson = +0.753, p<.001), which reinforces the bilateral symmetry of the antral plane morphology. The bilateral symmetry of the alveolonasal plane was supported by the positive association for this variable (Pearson = +0.503, p=.014).

Various studies have found that there is no significant difference between right and left MS volume [34,35], the MS volume in men is significantly larger than that of women [34,36], and MS volume decreases with increasing age [34]. Interestingly, such studies have not found or reported 33 any anatomic changes in typical MS geometry, such as sinus recesses [34-38]. When antral floor determinations have been performed, different variables of the dentosinus topography have been determined, but the lateral "sliding" of the superior FN from the maxillary alveolar base to the superior PM2 at the level of the PM2 has not been reported or studied [38-42]. It has been established that the mean adult maxillary sinus floor height correlates negatively with the volume of the MS and, in adults, is not significantly influenced by dentition status, increasing proportionally with decreasing zygomaticoalveolar ridge distance, as well as with height and body weight [43]. A study performed on both dentate and edentulous posterior maxillae concluded that, following tooth loss in the posterior maxilla, vertical bone height is lost mainly due to alveolar ridge resorption and not due to MS pneumatization [44]. In 321 randomly selected maxillary CBCT scans, MS alone was located above the maxillary second premolar in 46.9% [45]. In the study here [33], MS was exclusively localized above the maxillary alveolar base alone in 234/290 maxillary bones in types 1 and 2, for an overall prevalence of 80.68%. In types 1 and 2 that I determined here [33], both buccal (lateral) and transalveolar/transcrestal (inferior) antral plane approaches for schneiderian membrane elevation and endoosseous implant placement [46,47] could be utilized because they reach the antral plane. During transcrestal approaches, osteotomes may be initially directed palatally and then redirected more vertically to create the final osteotomy for implant placement [48]. However, if the antral-palatal wall is thin, the initial trajectory of the osteotome should be modified to engage a thicker area of the maxillary alveolar base [48]. In type 2, I determined the incidence of MS palatal recess, which was 11.72% on the right side and 15.17% on the left side, and correlated it with the vertical topography of the antral-palatal floor - higher than the nasal floor, at the same level as the nasal

floor and lower than the nasal floor [33]. Few studies have focused on such palatal recesses of the MS [49-51]. Different authors have considered palatal recesses as palatonasal recesses [47,49-52]. The antral-palatal wall of the antral plane has been considered to be the inferior side of the angle of the palatal recess angle; in such cases, the opening angle of the palatal recess has been determined as the angle between the antral-palatal wall and the sinonasal (medial) wall of the MS [47,51]. The palatine junction angle has been described as the angle between the palatine cortical plates of the antral-palatine wall of the antral-palatal floor and that of the palatine process of the maxillary bone [49,50]. In one of the available studies on the palatal recess of the MS, the authors found 1315 pneumatizations of different types, including the null, of the palatine processes, but, according to their claims, these resulted from only 188 cases (376 MS) [50]; this raises serious doubts about the veracity of these results. The same authors state that they assessed the 'gasification' of the palatine process of the maxillary sinus [50]. However, anatomically, the maxillary bone, and not the MS, anatomically projects several processes, including the palatine one. Apparently, closed palatine recesses of MS have not been previously found or described, which is explained by the rare occurrence of this type (0.69%). Neither the bilateral symmetry nor the asymmetry of palatal recess was determined when palatonasal recesses were found and measured [49]. In the present study we demonstrated that palatal recesses are not necessarily bilateral [33]. The incidence we found for palatal recessions is approximately half [33] of that previously found by Niu et al. (2018) They investigated many cases and found that at the premolar 2 and molar 1 sites, 62% of patients had no MS types of reccesses and 38% had palatonasal reccesses [47]. Palatal, or palatonasal, reccesses of MS have rarely been reported in the literature, and dentists should be aware of such normal morphology, as it could easily be mistaken for pathology [52].

The antral-palatal wall of the MS can be used for surgical sinus access and sinus lift (palatal window for sinus lift) [53]. Elevation of the antral floor through the antral-palatal wall of the MS allows for greater postoperative comfort, less postoperative edema, less marginal bone loss around implants and greater bone density around implants [53]. This approach may be used in cases with a deep palatal recess of the MS, thick buccal wall of the antral plane, or a prominent artery in the buccal wall that could be intercepted in the buccal bone window of the osteotomy [54]. Preoperative CBCT evaluation of patients helps surgeons decide whether to use palatal or buccal antral plateau elevation [53]. Furthermore, a preoperative scan would inform surgeons if anatomic conditions exist, such as in types 3 and 4 in the present study, to misdirect the palatal approach to the nasal fossa instead of MS [33]. In types 1 and 2, the medial wall of the

antral plain is a well-defined antral-palatal wall and was detected here in 80.69% of the investigated MSs. However, in 16.21% of sinuses, I found an alveolar base of type 3, in which the antral-palatal wall becomes a composite antral-palatal and nasal-palatal wall by widening of the nasal floor. In type 4 (3.10%), this wall is exclusively nasal-palatal. Therefore, in the palatal approach of the antral floor for sinus lift, these details should be known, cases should be anatomically evaluated preoperatively, and the erroneous approach of the nasal floor by this route can thus be avoided in patients with types 3 or 4 maxillary alveolar base [33]. In types 3 and 4, the maxillary alveolar base contributed to a nasal-palatal wall instead of an antral-palatal wall on 25/290 sides of the study group, or 8.62% [33]. The nasal-palatal bone could be utilized for implant placement, and if severely resorbed, a nasal floor elevation technique could be considered to increase the available bone [33]. The nasal elevation technique combines turbinectomy and elevation of the antero-posterior nasal floor through a lateral window using autogenous bone or bone substitutes to augment an atrophied alveolar ridge in the anterior maxilla 56. INM pneumatization increases the volume of the FN and results in displacement of the MS laterally and the FN inferiorly toward the posterior maxillary teeth [33]; this has been described as the "big nose" variant [45], the incidence of which is reported to be approximately 3% [55]. It has also been reported as a rare case [56]. Here I found a higher incidence of 8.62% [33]. A previous study established that more implants appeared to penetrate the MS floor when panoramic radiographs were observed. However, in CBCT, it was demonstrated that some of the implants penetrated the nasal floor, as the pneumatization of the lower meatus extended to the area of the second molar [57]. Indeed, a hyperpneumatization of the INM could result in either a type 3 or a type 4 maxillary alveolar base and should be carefully checked in CBCT and not on panoramic radiographs [33]. Especially when the MS appears small, given that the FN occupies a wider area in that region, this detail can be used for accurate interpretation [58].

2.6 The floor of the maxillary sinus at the level of the second upper molar

The MS floor is a trough made inferiorly between the lateral walls and the sinonasal wall of the MS. Inferior to this is the maxillary alveolar bone (maxillary alveolar base) [33]. As stated previously [33], studies on the antral plateau have followed the dento-antral relationships assuming a unique possibility of localization of the MS superior to the maxillary alveolar base [33]. There is, however, the anatomic possibility of a dilated INM reaching above the alveolar base of maxilla [33]. Various anatomic factors such as nasal septal deviation, concha bullosa and pneumatization of the INM may affect the insertion of implants in the posterior maxilla [59]. The identification of the vertical relationship between the maxillary molars and the antral floor is

important in dental extractions, endosseous implant planning and other surgical interventions in the maxillofacial region [60]. Partially edentulous patients with inadequate bone height in the posterior maxilla can be predictably rehabilitated by augmentation of the lateral wall of the MS and subsequent implant placement [61]. However, sinus augmentation is defined by the observed variations in the anatomic presentation of the MS [61]. It was decided to perform a separate study of the topography of the maxillary alveolar base at the level of the maxillary second molar to observe whether it is also altered at this level by INM dilation. I utilized an archived retrospective batch of head CBCT scans of 180 cases. I determined the prevalence of three distinct types of antral plateau at the maxillary second molar level: type 1, antral, in which superior to the alveolar base was located exclusively the MS, type 2, antral with palatal recess of the MS, and type 3, antral and nasal, in which a dilated INM was located superior to the alveolar base.

Of the 180 cases investigated, 79 (43.89%) were male and 101 (56.11%) - female. Type 1 was the most frequently encountered, irrespective of which side of the median plane and sex. In the overall group I found 337/360 (93.61%) types 1, 14/360 (3.89%) types 2 and 9/360 (2.2%) types 3. In 3/180 cases (1.66%) I identified bilateral asymmetry of the determined types. There were 2 cases with type 1+type 2 combination in females and 1 case with type 1+type 3 combination in males. Type 1 showed bilateral symmetry in 92.78% of cases, type 2 in 3.33% of cases, type 3 in 2.22% of cases and bilateral asymmetry of types occurred in 1.67% of cases. In 3.89% of cases I identified type 2 of antral plane (MS with palatal recess) in the maxillary second molar and in 2.2%, type 3 in which the alveolar base came in direct relation to both the MS and the INM. The situation differs from that of the maxillary second premolar where type 2, MS with palatal recession was identified in 16.17% and type 3 antral and nasal in 14.49%. Moreover, in the second premolar I found type 4 exclusively nasal in 3.45% while in the second molar this morphologic possibility was not recorded. It logically follows that INM dilatation in the upper molar area is not a frequent event. However, it cannot be assumed by surgeons that the alveolar base in the second molar is always antral and the evaluation of the morphologic pattern should be followed preoperatively. Furthermore, upper M2 extraction can be performed as part of orthodontic treatment [62-64]. In the situation of a dilated INM and therefore an antral type 3 floor, the palatal root of the M2 could have a nasal rather than antral ratio, which means that the nasal floor perforation during extraction could be avoided. Limited information is available on the pneumatization of the NIM for the insertion of endosseous implants in the posterior maxilla [59]. A total of 560 endosseous maxillary implants inserted in 324 patients were

analyzed, of which 132 implants appeared on panoramic radiographs as penetrating the antral floor [59]. CBCT analysis showed that 106 implants in 65 patients penetrated the MS and 26 implants in 13 patients penetrated the FN due to INM pneumatization [59]. Of the 13 patients, 6 were smokers and 7 were non-smokers [59]. During surgical procedures, perforation of the nasal mucosa was observed in all 13 patients [59]. No postoperative nasal symptoms were reported [59]. The nasal mucosa at the level of the implants showed no inflammatory signs [59]. When the MS is small in size and alveolar bone resorption is severe, panoramic assessment may lead to overestimation of the available residual bone; therefore it should be reassessed three-dimensionally [58]. In the situation of a dilated INM, a perforation of the nasal floor cortex may lead to an oronasal fistula. An analysis of the topographic relationships between the maxillary molar apexes and the MS floor obtained 4 types: type 1, when the molar apexes do not contact the antral floor, type 2, when these apexes contact the antral floor, type 3, with 1 penetrating root in the cortex of the antral floor, and type 4. with two or more penetrating apices [65]. No observations were presented regarding the relationship of maxillary molars to the nasal floor that I identified as possible in my study.

2.7 Topographic variability of the canine fossa

The canine fossa (CF) was studied in 50 dry skulls [66]. In 80% of cases it was clearly detectable, less prominent in 12% and in 8% it was even absent 66. In 40% it had bilateral asymmetry, the left one being wider [66]. On the CF is inserted the elevator of the angle of the mouth [66]. But it seems that the depth of the CF decreases with age [67]. Therefore, the study of CF in dry skulls of unknown age is of limited relevance. The Caldwell-Luc surgical procedure (antrostomy) or radical antrostomy allows removal of the destroyed MS mucosa, with access into the MS through the CF from the anterior wall of the MS and through the syn-nasal wall at the level of the INM for drainage [68]. The two-pathway approach complicates surgery because it requires long and angled instruments; however, different sinus pathologies require extended surgical access into the MS [69]. On the other hand, CF access is an ancillary procedure when endoscopic endonasal access of typical MS fails [70].

I aimed to determine the topography of the CF superiorly to the upper premolars (first, PM1, and second, PM2) on the assumption that it does not invariably and completely correspond to the MS. I used a retrospective batch of 100 cases - archived CBCT scans of the head. 52 male and 48 female cases were used. I defined (Fig. 3) three possible types of CF topography in the two upper premolars (PM1 - premolar 1 and PM2, premolar 2): type 1 - CF localized exclusively in the anterolateral wall of the MS (antral type of CF), type 2 - CF

localized in the nasal wall (external wall of the INM, nasal type of CF) and type 3, CF of antral and nasal type, contributing by its upper segment to the MS demarcation and by its lower segment belonging to the external wall of the INM.

Fig. 2-1. Canine fossa types determined on coronal sections. A. type 1 antral; B. type 2, nasal; C: type 3 antral and nasal. 1. maxillary sinus; 2. nasal fossa (inferior nasal meatus); 3. canine fossa.

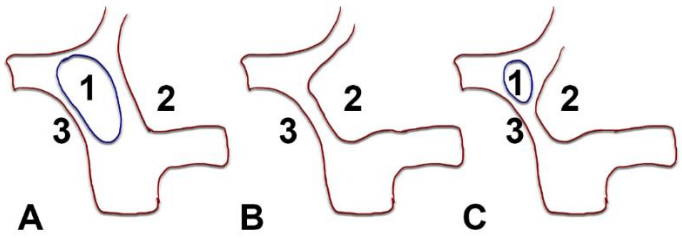

At PM1 on both sides of the median plane (n=200) CF type 1 was detected in 120 maxillae (60%), type 2 in 10 (5%) and type 3 in 70 maxillae (35%). I note that at PM1 on the left side, CF type 2 was not identified. At PM2 on both sides of the midplane (n=200), type 1 CF was detected in 119 maxillae (59.5%%), type 2 in 14 maxillary bones (7%) and type 3 in 67 maxillae (33.5%). I note that type 2 CF was not identified at PM2 on the left side. We determined (no. of cases, prevalences) in each upper premolar, 1 and 2, the combinations of types on both sides of the median plane (N=100 cases). At PM1 I did not identify bilateral (right/left) type 1/type 2, type 2/type 1, type 2/type 3 combinations. In PM2 there were no bilateral combinations including type 2 CF. Thus, at PM1 (N=100 cases) the bilateral (right/left) type 1/type 1 combination was detected in 35% of cases, type 1/type 3 in 6% of cases, type 2/type 2 in 10% of cases, type 3/type 1 in 4% of cases, type 3/type 2 in 4% of cases and type 3/type 3 in 41% of cases. At the PM1 level (N=100 cases) the bilateral (right/left) type 1/type 1 combination was detected in 74% of cases, type 1/type 3 in 5% of cases, type 3/type 1 in 6% of cases and type 3/type 3 in 15% of cases. In the group of 200 MS studied, I determined the number and prevalence of type 1-3 CF associations in PM1 and PM2. The type 1/PM1 + type 1/PM2 association was identified in 80/200 (40%) of sinuses. The type 2/PM1 + type 1/PM2 association was detected in 6/200 (3%) sinuses. Type 2/PM1 + type 3/PM2 association was detected in 18/200 (9%) sinuses. The association type 3/PM1 + type 1/PM2 was detected in 73/200 (36.5%) sinuses and the association between type 3/PM1 and type 3/PM2 was present in 23/200 (11.5%) sinuses. I present in the following graph the distribution of these associations on the right and left side. On the right, the type 1/1 (PM1/PM2) association was present in 41% of the cases, the 2/1 (PM1/PM2) association in 2% of the cases, the 2/3 PM1/PM2 association in 8% of the cases, the 3/1 (PM1/PM2) association in 36% of the cases and the 3/3 (PM1/PM2)

association in 13% of the cases. On the left, the 1/1 (PM1/PM2) type association was present in 39% of cases, the 2/1 (PM1/PM2) association in 4% of cases, the 2/3 PM1/PM2 association in 10% of cases, the 3/1 (PM1/PM2) association in 37% of cases and the 3/3 (PM1/PM2) association in 10% of cases. I found neither unilateral nor bilateral type 2/type 2, type 1/type 2 and type 1/type 3 (PM1/PM2) associated combinations in either sex.

As can be seen in the following graph, the gender distribution of CF type associations in upper premolars was relatively balanced.

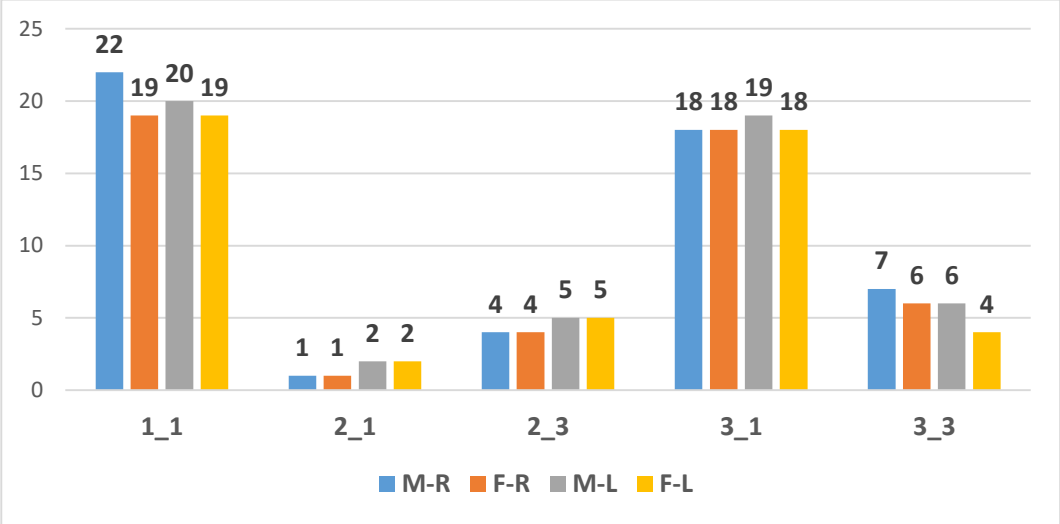

Graph 1. Part and sex distribution of associated unilateral combinations (type_/type_ at PM1/PM2). Number of cases. M: male; F: female; R: right side; L: left side.

In the overall group (N=100) I identified bilateral (right/left) morphologically symmetrical and asymmetrical combinations. Among the morphologically symmetrical, the 1_1/1_1_1 combination was present in 35% of the cases, the 3_1_1/3_1 combination in 27% of the cases, the 2_3/2_3 combination in 8%, the 3_3/3/3_3 combination in 7% of the cases and the 2_1_1/2_1 combination in only 2% of the cases. Asymmetric combinations were: 1_1_1/3_1 in 5% of cases, 3_3/3_1 in 5%, 3_1/1_1 in 3%, 3_1/2_1 in 2%, 3_1/2_1 in 2%, 3_1/2_3 in 2%, 3_1/3_3 in 2%, 1_1/3_3 in 1% and 3_3/1_1 in 1% of cases.

CF formation is the combined effect of genetic and various epigenetic influences. It could be directly related to sexual dimorphism, being more prevalent in male than female individuals, of human groups that have lived in tropical and high-altitude environments. The epigenetics of CF warrants future systematic study, including considerations of embryology, growth and development, developmental plasticity and modularity [71]. The definition of CF has evolved, reflecting its anatomical complexity and evolutionary significance. Traditionally it has been described as an infraorbital depression largely covering the maxillary zygomatic process

[72]. White et al. (2012) describe it as a variable cavity located below the infraorbital foramen [73], Lieberman (2011) defines it as a vertical depression above the root of the canine [74], and Jeon et al. (2017) localizes it lateral to the canine crest [67], similar to Schaitkin (2010) [75]. A modern definition reinforces these perspectives: the CF is a depression of variable extent located in the anterior maxilla, below the infraorbital foramen, lateral to the canine crest, recognizing the anatomical diversity of this structure [71]. My results support that a hypoplastic, short anterior and/or inferior MS can lead to altered CF topography. Hypoplastic MS (HMS), however, has been classified according to the alteration mainly of the anatomical structures of the lateral nasal wall. Bolger defined three types of MSH correlated with UP changes [76]. In type I MSH (6.9%) the PU has normal size and morphology, the EI is well defined and the degree of hypoplasia is mild; the degree of sinus involvement is variable [76]. In type II (3%), UP is absent or hypoplastic and EI is absent or ill-defined; sinus mucosal involvement is invariably present [76]. In type III (0.5%) PU is absent and sinus hypoplasia is marked [76]. MSH may also be accompanied by other morphological changes: orbital enlargement, sphenomaxillary plate, canine fossa elevation, widening of the inferior orbital fissure, thickening of the MS wall, hypo- or flattening of other sinuses, CEA variations, lateralization of the infraorbital canal, widening of the superior orbital fissure, widening of the pterygopalatine fossa or presence of an ethmomaxillary sinus [77,78]. Another study found MSH in 4.6% of cases (31 MSH), of which 54.8% were type I Bolger, 32.2% type II Bolger and 12.9% type III Bolger [77]. Mustian (1933) studied on dried skulls 100 human MS [79]. The author did not calculate prevalences for the different anatomical landmarks observed [79]. He noted that a CF that appears to approach the lateral nasal wall may be misleading [79]. In such cases, the MS either extends sagittally with a strip below the CF or ends abruptly immediately distal to the CF [79]. Therefore, to enter the MS through the CF it is preferable to approach the antero-lateral aspect of the zygomatic process [79]. This opening must be made high to avoid injury to the superior alveolar plexus and dental apices [79]. Topographically, this approach will be inferior and distal to the IOF, which will avoid the ION and IOA branches [79]. Mustian formulates a fairly reliable theorem that when the CF corresponds to the lateral nasal wall, the canine and premolars do not directly contact the MS [79], as is also evident from my research. In such cases, a misapplied force against these teeth will push them into either the CF or the INM [79]. An attempt to open the MS via the CF will create an opening of the INM [79].

Anand et al. (2008) detail the anterior wall trepanation "on the lateral side of the FC, immediately above the root of the canine and premolars" [70]. Anatomically, the approach

superior to the canine root intercepts the ampulla of the sinuous canal located at the CNI insertion into the lateral nasal wall. On the other hand, the CF approach above PM1, as shown in my study, may direct the surgically inserted trocar into the INM and not into the MS. It is unclear why the respective authors localize the lateral portion of the CF above the canine; this would anatomically mislocalize the medial aspect of the CF superior to the maxillary incisors.

Various surgical studies of CF refer to the CF puncture technique [80-89]. Petersen (1981) describes the CF puncture technique as follows: the superior buccal sulcus is used and the center of CF is punctured a few millimeters superior to the dental apex [89]. The author does not explicitly indicate which maxillary teeth he is referring to, and does not consider the possibility of variation in their root length. Lee (2010) only indicates that a microdebrider was inserted into the MS by puncturing the CF [85]. Elidan et al. (1983) did not indicate anatomic landmarks for puncturing CF [83]. Sathananthar et al. (2005) repeat the CF at the intersection of the midpupillary line and a horizontal line tangent to the inferior border of the nasal ala [90]. These landmarks do not, however, define the position of the CF relative to the maxillary premolars, nor do they exclude the possibility of trocar entry into the INM. Albu et al. (2011) inserted the trocar in the CF superior and lateral to the maxillary canine root, thus superior to PM1, at the intersection of a vertical line through the pupil (exact pupil location not specified) and a horizontal line through the nasal floor (no explicit reference to the nasal wing) [80]. The landmarks described by Albu et al. (2011) were also previously used by Singhal et al. (2007) [91]. Seiberling et al. (2009) [92] also used the landmarks described by Singhal et al. (Byun and Lee (2011, 2013, 2014) and Lee et al. (2009) used the mediopupillary line and the horizontal line through the inferior contour of the nasal inferior wing as landmarks for CF puncture [81,82,93,94], described by Sathananthar et al. (Schaitkin (2010) finds the CF at the intersection of the mediopupillary line with a line "from the nasal vestibule" [75]. Feldt et al. (2011) find the CF using the mediopupillary line and the 'nasal floor' [69]. Robinson and Wormald (2005) show the CF landmark at the intersection of the mediopupillary line and the horizontal line through the "piriform aperture floor" [95].

CF types 2 and 3 respectively correspond to a dilated INM to a possibly low volume MS. Thus, endoscopic medial maxillectomy for endosinusal approach, if decided in such cases, should be carefully directed into the sinus cavity avoiding the CF directly into the superior vestibular groove. Localization of the CF in the INM wall recommends preoperative imaging evaluation prior to MS approach via the CF pathway, either for endoscopy or even just for fossa

puncture. CF localization distal to the canine ridge does not exclude the possibility that this fossa may be located in the lateral wall of the INM at the level of the maxillary first premolar.

2.8 Sinusurile etmomaxilare

Functional endoscopic surgery of the paranasal sinuses is constantly benefiting from good anatomical knowledge and modern imaging techniques. These allow precise preoperative identification of ethmoid air cells migrating to specific topographic sites near the ethmoid. The posterior ethmoid cells descending into the MS are the ethmoaxillary sinuses (EMS). They drain into the upper nasal meatus and have been found in 0.68-16.48% in the few previous studies. While infraorbital Haller's cells are anterior ethmoid cells that approach the ethmoid infundibulum, SEMs differ from Haller's cells. A posterior ethmoid cell sandwiched between the ethmoid, MS, and SphenS is a Sieur cell, but could also be considered a SEM. An SEM should be discriminated from a maxillary recess of the SphenS. However, an SEM could determine the maxillary bulla of Onodi. A deduplicated false MS, described by Zuckerkandl, is a MS draining into the middle nasal meatus, posteriorly contiguous with a SEM draining into the upper nasal meatus. These are separated by the ethmoaxillary septum, which may be mistaken for a MS septum if the drainage pathways are not accurately documented by computed tomography. Therefore, a case-by-case anatomic identification of the pneumatic spaces near the MS should be performed prior to endoscopic surgical approaches of the nose and sinuses [96].

3 Conclusions of the doctoral thesis

1. Because all morphologic possibilities of the nasal septum involve the uPEPr portion of the PEP are located in the uPEPr, narrow portion of the nasal cavity. Therefore they must be appropriately differentiated during surgical approaches of the nasal septum and the ridged blade of the ethmoid. Being extended from neighboring paranasal sinuses, PEP and CG pneumatizations may trigger clinical pictures of their pneumatization sources.
2. When surgically approaching the posterior ethmoid and sphenoid sinus, care must be taken to accurately identify any pneumatization of the PEC to avoid using the wrong surgical corridors leading to undesirable events.
3. Varying antral-palatal wall ratios with the MS and NF should be evaluated preoperatively to prevent erroneous surgical access in the NF and not in the MS.

4. The maxillary sinus is not an exclusive possibility for pneumatization of the maxillary bone. Posterior ethmoid cells draining into the SNM could migrate superiorly and/or posteriorly to the SNM with different morphologic and topographic patterns.
5. The retrobulbar recess of the SNM is a proven anatomic variant and therefore the origin of a retrobulbar pneumatization should be carefully documented by imaging if surgical approaches of the nasal lateral wall are intended.
6. The maxillary alveolar bone in the area of the maxillary 2nd premolar should not be considered exclusively subantral during surgical approaches to the maxillary sinus floor or when learning specific anatomy for dentistry.
7. It cannot be assumed by surgeons that the alveolar base of the maxillary second molar is always antral and the morphologic pattern assesMSent should be followed preoperatively, although dilatation of the lower nasal meatus is rare at this level.
8. When dilatation of the inferior nasal meatus is identified with its localization superior to the edentulous alveolar bone, elevation of the nasal floor instead of the antral floor with simultaneous insertion of endosseous implants may be practiced.
9. The anatomic drainage pathway to the nasal fossa allows discrimination between different paranasal pneumatizations, including between a sphenoethmoid cell (Onodi) and the sphenoid sinus.
10. The possibility of localization of the canine fossa in the lateral wall of the inferior nasal meatus recommends careful preoperative imaging evaluation when either approaching the maxillary sinus via the inferior nasal meatus or puncturing or trepanation of the canine fossa for surgical penetration of the maxillary sinus is intended.

Bibliografie

1. Kowalczyk KA, Majewski A. Analysis of surgical errors associated with anatomical variations clinically relevant in general surgery. Review of the literature. *Transl Res Anat* 2021; **23**: 100107.
2. Vasvari G, Reisch R, Patonay L. Surgical anatomy of the cribriform plate and adjacent areas. *Minimally invasive neurosurgery : MIN* 2005; **48**(1): 25-33.
3. Muresan AN, Rusu MC, Radoi PM, Toader C. Patterns of Pneumatization of the Posterior Nasal Roof. *Tomography* 2022; **8**(1): 316-28.
4. Van Alyea O. Ethmoid labyrinth: anatomic study, with consideration of the clinical significance of its structural characteristics. *Arch Otolaryngol* 1939; **29**(6): 881-902.
5. Van Alyea OE. Sphenoid sinus: anatomic study, with consideration of the clinical significance of the structural characteristics of the sphenoid sinus. *Arch Otolaryngol* 1941; **34**(2): 225-53.
6. Wang J, Bidari S, Inoue K, Yang H, Rhoton A, Jr. Extensions of the sphenoid sinus: a new classification. *Neurosurgery* 2010; **66**(4): 797-816.
7. Yanagisawa E, Weaver EM, Ashikawa R. The Onodi (sphenoethmoid) Cell. *Ear Nose Throat J* 1998; **77**(8): 578-80.
8. Kainz J, Stammberger H. Danger areas of the posterior rhinobasis. An endoscopic and anatomical-surgical study. *Acta oto-laryngologica* 1992; **112**(5): 852-61.
9. Çalışkan A, Sumer AP, Bulut E. Evaluation of anatomical variations of the nasal cavity and ethmoidal complex on cone-beam computed tomography. *Oral Radiol* 2017; **33**(1): 51-9.
10. Pedziwiatr ZF. Structural pattern of the ethmoidal labyrinth in adult man. II. *Archiv fur klinische und experimentelle Ohren- Nasen- und Kehlkopfheilkunde* 1973; **204**(1): 8-16.
11. Rusu MC, Sandulescu M, Derjac-Arama AI. The pterygopalatine recess of the superior nasal meatus. *Surgical and radiologic anatomy : SRA* 2016; **38**(8): 979-82.
12. Rusu MC, Sava CJ, Ilie AC, Sandulescu M, Dinca D. Agger Nasi Cells Versus Lacrimal Cells and Uncinate Bullae in Cone-Beam Computed Tomography. *Ear Nose Throat J* 2019; **98**(6): 334-9.
13. Sava CJ, Rusu MC, Sandulescu M, Dinca D. Vertical and sagittal combinations of concha bullosa media and paradoxical middle turbinate. *Surg Radiol Anat* 2018; **40**(7): 847-53.
14. Kaplanoglu H, Kaplanoglu V, Dilli A, Toprak U, Hekimoglu B. An analysis of the anatomic variations of the paranasal sinuses and ethmoid roof using computed tomography. *The Eurasian journal of medicine* 2013; **45**(2): 115-25.
15. Marquez S, Tessema B, Clement PA, Schaefer SD. Development of the ethmoid sinus and extramural migration: the anatomical basis of this paranasal sinus. *Anatomical record* 2008; **291**(11): 1535-53.
16. Basic N, Basic V, Jukic T, Basic M, Jelic M, Hat J. Computed tomographic imaging to determine the frequency of anatomical variations in pneumatization of the ethmoid bone. *European archives of oto-rhino-laryngology : official journal of the European Federation of Oto-Rhino-Laryngological Societies* 1999; **256**(2): 69-71.
17. Meloni F, Mini R, Rovasio S, Stomeo F, Teatini GP. Anatomic variations of surgical importance in ethmoid labyrinth and sphenoid sinus. A study of radiological anatomy. *Surgical and radiologic anatomy : SRA* 1992; **14**(1): 65-70.
18. Kantarci M, Karasen RM, Alper F, Onbas O, Okur A, Karaman A. Remarkable anatomic variations in paranasal sinus region and their clinical importance. *European journal of radiology* 2004; **50**(3): 296-302.
19. von Arx T, Lozanoff S, Bornstein MM. Extraoral anatomy in CBCT - a literature review. Part 1: Nasoethmoidal region. *Swiss dental journal* 2019; **129**(10): 804-15.
20. Gore MR. The supraseptal ethmoid sinus cell: A previously unreported ethmoid sinus variant. *Clin Case Rep* 2019; **7**(7): 1306-8.
21. Yin LX, Low CM, Puccinelli CL, et al. Olfactory outcomes after endoscopic skull base surgery: A systematic review and meta-analysis. *The Laryngoscope* 2019; **129**(9): 1998-2007.
22. Yanagisawa E. Endoscopic view of sphenoethmoidal recess and superior meatus. *Ear Nose Throat J* 1993; **72**(5): 331-2.
23. Castle-Kirszbaum M, Uren B, Goldschlager T. Anatomic Variation for the Endoscopic Endonasal Transsphenoidal Approach. *World neurosurgery* 2021; **156**: 111-9.

24. Majmundar N, Kamal NH, Reddy RK, Eloy JA, Liu JK. Limitations of the endoscopic endonasal transcribriform approach. *Journal of neurosurgical sciences* 2018; **62**(3): 287-96.
25. Rusu MC, Muresan AN, Dandoczi CA, Vrapciu AD. Middle meatal nasal recesses of the maxillary sinuses and dangerously modified nasal anatomy. *Anatomy & cell biology* 2024.
26. Muresan AN, Mogoanta CA, Stanescu R, Rusu MC. The sinus septi nasi and other minor pneumatizations of the nasal septum. *Rom J Morphol Embryol* 2021; **62**(1): 227-31.
27. Kaban Y, Coskun Z, Akar B. A Systematic Literature Study of the Sinus Septi Nasi, Crista Galli and Other Minor Pneumatizations. *Int J Morphol* 2023; **1**(2): 2.
28. Liu J, Wang Y, Yan Z, Yang Y. Anatomical identification of supraseptal posterior ethmoid cells and its significance for endoscopic sinus surgery. *Folia Morphol (Warsz)* 2023; **82**(3): 696-703.
29. Kilic C, Kamburoglu K, Yuksel SP, Ozen T. An Assessment of the Relationship between the Maxillary Sinus Floor and the Maxillary Posterior Teeth Root Tips Using Dental Cone-beam Computerized Tomography. *European journal of dentistry* 2010; **4**(4): 462-7.
30. Shokri A, Lari S, Yousef F, Hashemi L. Assessment of the relationship between the maxillary sinus floor and maxillary posterior teeth roots using cone beam computed tomography. *The journal of contemporary dental practice* 2014; **15**(5): 618-22.
31. Kang SH, Kim BS, Kim Y. Proximity of Posterior Teeth to the Maxillary Sinus and Buccal Bone Thickness: A Biometric Assessment Using Cone-beam Computed Tomography. *Journal of endodontics* 2015; **41**(11): 1839-46.
32. Nimigean V, Nimigean VR, Maru N, Salavastru DI, Badita D, Tuculina MJ. The maxillary sinus floor in the oral implantology. *Romanian journal of morphology and embryology = Revue roumaine de morphologie et embryologie* 2008; **49**(4): 485-9.
33. Muresan AN, Dandoczi CA, Tudose RC, Hostiuc S, Rusu MC. Anatomical Possibilities of the Alveolar Bone at the Upper Second Premolar Level. *Medicina (Kaunas)* 2024; **60**(5).
34. Aktuna Belgin C, Colak M, Adiguzel O, Akkus Z, Orhan K. Three-dimensional evaluation of maxillary sinus volume in different age and sex groups using CBCT. *European archives of oto-rhino-laryngology : official journal of the European Federation of Oto-Rhino-Laryngological Societies* 2019; **276**(5): 1493-9.
35. Sarilita E, Lita YA, Nugraha HG, Murniati N, Yusuf HY. Volumetric growth analysis of maxillary sinus using computed tomography scan segmentation: a pilot study of Indonesian population. *Anatomy & cell biology* 2021; **54**(4): 431-5.
36. Sharma SK, Jehan M, Kumar A. Measurements of maxillary sinus volume and dimensions by computed tomography scan for gender determination. *J Anat Soc India* 2014; **63**(1): 36-42.
37. Tolstunov L, Thai D, Arellano L, . Implant-guided volumetric analysis of edentulous maxillary bone with cone-beam computerized tomography scan. Maxillary sinus pneumatization classification. *The Journal of oral implantology* 2012; **38**(4): 377-90.
38. Gu Y, Sun C, Wu D, Zhu Q, Leng D, Zhou Y. Evaluation of the relationship between maxillary posterior teeth and the maxillary sinus floor using cone-beam computed tomography. *BMC oral health* 2018; **18**(1): 164.
39. Kwak HH, Park HD, Yoon HR, Kang MK, Koh KS, Kim HJ. Topographic anatomy of the inferior wall of the maxillary sinus in Koreans. *International journal of oral and maxillofacial surgery* 2004; **33**(4): 382-8.
40. Ok E, Gungor E, Colak M, Altunsoy M, Nur BG, Aglarci OS. Evaluation of the relationship between the maxillary posterior teeth and the sinus floor using cone-beam computed tomography. *Surg Radiol Anat* 2014; **36**(9): 907-14.
41. Razumova S, Brago A, Howijieh A, Manvelyan A, Barakat H, Baykulova M. Evaluation of the relationship between the maxillary sinus floor and the root apices of the maxillary posterior teeth using cone-beam computed tomographic scanning. *Journal of conservative dentistry : JCD* 2019; **22**(2): 139-43.
42. Yoshimine S, Nishihara K, Nozoe E, Yoshimine M, Nakamura N. Topographic analysis of maxillary premolars and molars and maxillary sinus using cone beam computed tomography. *Implant dentistry* 2012; **21**(6): 528-35.
43. Ariji Y, Ariji E, Yoshiura K, Kanda S. Computed tomographic indices for maxillary sinus size in comparison with the sinus volume. *Dento maxillo facial radiology* 1996; **25**(1): 19-24.
44. Schriber M, Bornstein MM, Suter VGA. Is the pneumatisation of the maxillary sinus following tooth loss a reality? A retrospective analysis using cone beam computed tomography and a customised software program. *Clinical oral investigations* 2019; **23**(3): 1349-58.
45. Haj Yahya B, Bar-Hai D, Samehov D, Chaushu G, Hamzani Y. Sinus Augmentation-Expect the Unexpected: Diagnostic Anatomical Study. *Journal of clinical medicine* 2021; **10**(19): 4293.

46. Albadani MM, Elayah SA, Al-Wesabi MA, Al-Aroomi OA, Al Qadasy NE, Saleh H. A graftless maxillary sinus lifting approach with simultaneous dental implant placement: a prospective clinical study. *BMC oral health* 2024; **24**(1): 227.
47. Niu L, Wang J, Yu H, Qiu L. New classification of maxillary sinus contours and its relation to sinus floor elevation surgery. *Clinical implant dentistry and related research* 2018; **20**(4): 493-500.
48. Bruschi GB, Bruschi E, Papetti L. Flapless Localised Management of Sinus Floor (LMSF) for trans-crestal sinus floor augmentation and simultaneous implant placement. A retrospective non-randomized study: 5-year of follow-up. *Heliyon* 2021; **7**(9): e07927.
49. Serindere G, Serindere M, Gunduz K. Evaluation of maxillary palatal process pneumatization by cone-beam computed tomography. *Journal of stomatology, oral and maxillofacial surgery* 2023; **124**(4): 101432.
50. Gunacar DN, Kose TE, Arsan B, Aydin EZ. Radioanatomic study of maxillary sinus palatal process pneumatization. *Oral Radiol* 2022; **38**(3): 398-404.
51. Chan HL, Monje A, Suarez F, Benavides E, Wang HL. Palatonasal Recess on Medial Wall of the Maxillary Sinus and Clinical Implications for Sinus Augmentation via Lateral Window Approach. *Journal of periodontology* 2013; **84**: 1087-93.
52. Omami G. Palatine recess of maxillary sinus masquerading as radiolucent lesion: case report. *Libyan Dent J* 2013; (3).
53. EL-prince ON, Khalil AF, EL-sabbagh AM, Fahmy MH. Palatal Versus Buccal Antral Approach for Maxillary Sinus Lifting and Implant Placement. *Alexandria Dent J* 2018; **43**(2): 39-45.
54. Rahpeyma A, Khajehahmadi S. Indications for palatal sinus lift: Case series. *Journal of Indian Society of Periodontology* 2018; **22**(3): 254-6.
55. Misch CE, Resnik R. Misch's avoiding complications in oral implantology. St. Louis, Missouri: Elsevier Health Sciences; 2017.
56. Khoshhal M, Vafaee F, Sabounchi SS, Sabounchi SS. Three-dimensional radiograph revealing the big-nose variant before dental implant surgery in posterior maxilla: A rare case report. *Int J Med Res Prof* 2016; **2**(4): 132-4.
57. Park WB, Kim YJ, Kang KL, Lim HC, Han JY. Long-term outcomes of the implants accidentally protruding into nasal cavity extended to posterior maxilla due to inferior meatus pneumatization. *Clinical implant dentistry and related research* 2020; **22**(1): 105-11.
58. Yeom HG, Huh KH, Yi WJ, et al. Nasal cavity perforation by implant fixtures: case series with emphasis on panoramic imaging of nasal cavity extending posteriorly. *Head & face medicine* 2023; **19**(1): 37.
59. Park WB, Kim YJ, Kang KL, Lim HC, Han JY. Long-term outcomes of the implants accidentally protruding into nasal cavity extended to posterior maxilla due to inferior meatus pneumatization. *Clinical implant dentistry and related research* 2020; **22**(1): 105-11.
60. Swathi K, Maragathavalli G. Assessment of the vertical relationship between the maxillary posterior teeth and the maxillary antral floor in a South Indian population using Cone Beam Computed Tomography-A radiographic observational study. *Biomedicine / [publiee pour l'AAICIG]* 2022; **42**(3): 499-503.
61. Park WB, Crasto GJ, Park W, Han JY, Kang P. Successful Implant Placement via Simultaneous Nasal Floor Augmentation in an Inferior Meatus Pneumatization Case. *Medicina (Kaunas)* 2023; **59**(2).
62. Bishara SE, Ortho D, Burkey PS. Second molar extractions: a review. *Am J Orthod* 1986; **89**(5): 415-24.
63. Anderson RH. A review of second molar extractions in orthodontics. *J Gen Orthod* 1992; **3**(4): 26-7.
64. Lee W, Wong RW, Ikegami T, Hagg U. Maxillary second molar extractions in orthodontic treatment. *World journal of orthodontics* 2008; **9**(1): 52-61.
65. Yalcin M, Lacin N. Is the relationship of maxillary molar roots to the floor of the maxillary sinus associated with antral pseudocysts? A retrospective study using cone beam computed tomography. *Oral surgery, oral medicine, oral pathology and oral radiology* 2020; **130**(5): 574-82.
66. Stan MC, Bordei P, Dina C, Iliescu D. Characteristics of some anatomical landmarks on the anterior face of the maxilla. *ARS Medica Tomitana* 2013; **19**(2): 79-83.
67. Jeon A, Sung KH, Kim SD, et al. Anatomical changes in the East Asian midface skeleton with aging. *Folia Morphol (Warsz)* 2017; **76**(4): 730-5.
68. Huang YC, Chen WH. Caldwell-Luc operation without inferior meatal antrostomy: a retrospective study of 50 cases. *Journal of oral and maxillofacial surgery : official journal of the American Association of Oral and Maxillofacial Surgeons* 2012; **70**(9): 2080-4.
69. Feldt BA, McMains KC, Weitzel EK. Cadaveric comparison of canine fossa vs transnasal maxillary sinus access. *International forum of allergy & rhinology* 2011; **1**(3): 183-6.

70. Anand V, Santosh S, Aishwarya A. Canine fossa approaches in endoscopic sinus surgery - our experience. *Indian journal of otolaryngology and head and neck surgery : official publication of the Association of Otolaryngologists of India* 2008; **60**(3): 214-7.
71. Ribot F, Bartual M, Enciso AJ, Wang Q. The canine fossa and the evolution of the midface in humans. *Acta Anthropol Sin* 2020: 191-227.
72. Mellinger WJ. The Canine Fossa. *Archives of otolaryngology* 1940; **31**(6): 930-7.
73. White TD, Black MT, Folkens PA. Human osteology: Third edition: Elsevier; 2011.
74. Lieberman DE. The Evolution of the Human Head: The Belknap Press of Harvard University Press; 2011.
75. Schaitkin B. Canine fossa puncture: Safe visualization of the recesses of the maxillary sinus. *Oper Techn Otolaryngol Head Neck Surg* 2010; **21**(3): 160-2.
76. Bolger WE, Woodruff WW, Jr., Morehead J, Parsons DS. Maxillary sinus hypoplasia: classification and description of associated uncinate process hypoplasia. *Otolaryngology--head and neck surgery : official journal of American Academy of Otolaryngology-Head and Neck Surgery* 1990; **103**(5 (Pt 1)): 759-65.
77. Selcuk A, Ozcan KM, Akdogan O, Bilal N, Dere H. Variations of maxillary sinus and accompanying anatomical and pathological structures. *The Journal of craniofacial surgery* 2008; **19**(1): 159-64.
78. Geraghty JJ, Dolan KD. Computed tomography of the hypoplastic maxillary sinus. *The Annals of otology, rhinology, and laryngology* 1989; **98**(11): 916-8.
79. Mustian WF. The floor of the maxillary sinus and its dental, oral and nasal relations. *Journal of the American Dental Association* 1933; **20**(12): 2175-87.
80. Albu S, Baciut M, Opincariu I, Rotaru H, Dinu C. The canine fossa puncture technique in chronic odontogenic maxillary sinusitis. *American journal of rhinology & allergy* 2011; **25**(5): 358-62.
81. Byun JY, Lee JY. Canine fossa puncture for severe maxillary disease in unilateral chronic sinusitis with nasal polyp. *The Laryngoscope* 2013; **123**(12): E79-84.
82. Byun JY, Lee JY, Baek BJ. Weakness of buccal branch of facial nerve after canine fossa puncture. *The Journal of laryngology and otology* 2011; **125**(2): 214-6.
83. Elidan J, Gay I, Chisin R. Irrigation of the maxillary sinus by canine fossa puncture. Experience with 202 patients. *The Annals of otology, rhinology, and laryngology* 1983; **92**(5 Pt 1): 528-9.
84. Katholm M, Brofeldt S. Canine fossa puncture: an alternative to antro-nasal puncture of the maxillary sinus. *Ear Nose Throat J* 1991; **70**(5): 325-6.
85. Lee JH. Canine fossa puncture along with endonasal endoscopy for the management of fungal balls in the maxillary sinus. *Clinical otolaryngology : official journal of ENT-UK ; official journal of Netherlands Society for Oto-Rhino-Laryngology & Cervico-Facial Surgery* 2010; **35**(6): 512-3.
86. Lee JY, Lee SH, Hong HS, Lee JD, Cho SH. Is the canine fossa puncture approach really necessary for the severely diseased maxillary sinus during endoscopic sinus surgery? *The Laryngoscope* 2008; **118**(6): 1082-7.
87. Neves-Pinto RM, Medrado AC, da Silva CA, Palis W. Puncture in the canine fossa: technique and pros and cons. *Rhinology* 1982; **20**(1): 41-8.
88. Petersen RJ. Canine fossa puncture. *The Laryngoscope* 1973; **83**(3): 369-71.
89. Petersen RJ. "How I do it"--head and neck. A targeted problem and its solution. Sinus puncture therapy: canine fossa puncture method. *The Laryngoscope* 1981; **91**(12): 2126-8.
90. Sathananthar S, Nagaonkar S, Paleri V, Le T, Robinson S, Wormald PJ. Canine fossa puncture and clearance of the maxillary sinus for the severely diseased maxillary sinus. *The Laryngoscope* 2005; **115**(6): 1026-9.
91. Singhal D, Douglas R, Robinson S, Wormald PJ. The incidence of complications using new landmarks and a modified technique of canine fossa puncture. *American journal of rhinology* 2007; **21**(3): 316-9.
92. Seiberling K, Ooi E, MiinYip J, Wormald PJ. Canine fossa trephine for the severely diseased maxillary sinus. *American journal of rhinology & allergy* 2009; **23**(6): 615-8.
93. Byun JY, Lee JY. Effect of maxillary sinus packing with epinephrine hydrochloride-soaked cotton pledgets on complications after canine fossa puncture. *Acta oto-laryngologica* 2014; **134**(3): 300-6.
94. Lee JY, Baek BJ, Kim DW, Byun JY, Lee SW, Hong HS. Changes in the maxillary sinus volume and the surgical outcome after the canine fossa puncture approach in pediatric patients with an antrochoanal polyp: results of a minimum 3-year follow-up. *American journal of rhinology & allergy* 2009; **23**(5): 531-4.
95. Robinson S, Wormald PJ. Patterns of innervation of the anterior maxilla: a cadaver study with relevance to canine fossa puncture of the maxillary sinus. *The Laryngoscope* 2005; **115**(10): 1785-8.
96. Geamanu A, Rusu MC, Muresan AN, Vrapciu AD. The Ethmomaxillary Sinus-A False Duplicate Maxillary Sinus. *The Journal of craniofacial surgery* 2024; **35**(5): e458-e61.